Article

Hydrogen Production under Aerobic Conditions by Membrane-Bound Hydrogenases from Ralstonia Species

Gabrielle Goldet, Annemarie F. Wait, James A. Cracknell, Kylie A. Vincent, Marcus Ludwig, Oliver Lenz, Ba#rbel Friedrich, and Fraser A. Armstrong

J. Am. Chem. Soc., **2008**, 130 (33), 11106-11113 • DOI: 10.1021/ja8027668 • Publication Date (Web): 29 July 2008

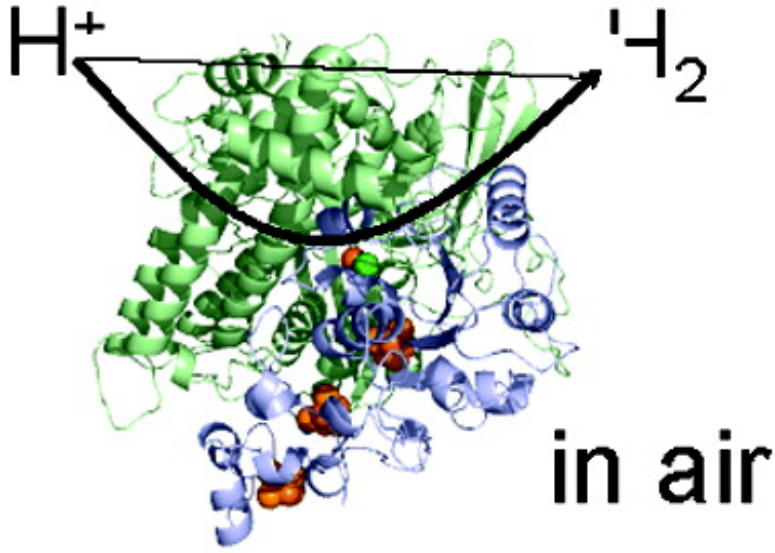

More About This Article

Additional resources and features associated with this article are available within the HTML version:

- Supporting Information
- Access to high resolution figures
- Links to articles and content related to this article
- Copyright permission to reproduce figures and/or text from this article

View the Full Text HTML

Journal of the American Chemical Society is published by the American Chemical Society. 1155 Sixteenth Street N.W., Washington, DC 20036

J|A|C|S
ARTICLES

Published on Web 07/29/2008

Hydrogen Production under Aerobic Conditions by Membrane-Bound Hydrogenases from *Ralstonia* Species

Gabrielle Goldet,[†] Annemarie F. Wait,[†] James A. Cracknell,[†] Kylie A. Vincent,[†] Marcus Ludwig,[‡] Oliver Lenz,[‡] Bärbel Friedrich,[‡] and Fraser A. Armstrong*[,†]

Inorganic Chemistry Laboratory, Department of Chemistry, University of Oxford, South Parks Road, Oxford OX1 3QR, United Kingdom, and Institut für Biologie/Mikrobiologie, Humboldt-Universität zu Berlin, Chausseestrasse 117, 10115 Berlin, Germany

Received April 15, 2008; E-mail: fraser.armstrong@chem.ox.ac.uk

Abstract: Studies have been carried out to establish the ability of O_2-tolerant membrane-bound [NiFe] hydrogenases (MBH) from *Ralstonia* sp. to catalyze H_2 production in addition to H_2 oxidation. These hydrogenases are not noted for H_2-evolution activity, and this is partly due to strong product inhibition. However, when adsorbed on a rotating disk graphite electrode the enzymes produce H_2 efficiently, provided the H_2 product is continuously removed by rapidly rotating the electrode and flowing N_2 through the gastight electrochemical cell. Electrocatalytic H_2 production proceeds with minimal overpotential—a significant observation because lowering the overpotential (the electrochemically responsive activation barrier) is seen as crucial in developing small-molecule catalysts for H_2 production. A mutant having a high K_M for H_2 oxidation did not prove to be a better H_2 producer relative to the wild type, thus suggesting that weak binding of H_2 does not itself confer a tendency to be a H_2 producer. Inhibition by H_2 is much stronger than inhibition by CO and, most significantly, even O_2. Consequently, H_2 can be produced sustainably in the presence of O_2 as long as the H_2 is removed continuously, thereby proving the feasibility for biological H_2 production in air.

Introduction

There is increasing interest in H_2 production from renewable resources,[1] and "biological H_2" is one promising approach, either directly, via microorganisms (photosynthetic[2–6] or fermentative[7] hydrogen farms), or via new catalysts, devoid of precious metals, that are inspired by enzymes.[8–18] Hydrogenases are metalloenzymes, widespread throughout the microbial world, with active sites consisting of first-row transition metals (Fe, or Fe and Ni) coordinated by thiolates and diatomic ligands (CN^- and CO). The two main classes, known as [FeFe]- and [NiFe]-hydrogenases, catalyze the rapid interconversion of H_2 and H^+ (water or H^+_{aq}). These two classes differ in active-site composition and share no sequence similarity; indeed, they are considered products of convergent evolution, such was (and remains) the importance of H_2-based metabolism and energy cycling to biology.[1] The structure of the active site of a [NiFe] hydrogenase is shown in Figure 1.

The minimal common structural fragment, [(RS)Fe(CO)], found in all hydrogenases isolated so far, is significant because in the enzyme it forms the basis of a catalyst that is probably at least as active as Pt-based centers.[20–22] Not surprisingly, therefore, understanding, exploiting, and mimicking the catalytic properties of hydrogenases are important challenges with great significance for the future of H_2 as an energy carrier.[1,3] Although hydrogenases are very active enzymes for cycling H_2 and H^+, they are generally found to be inactivated by O_2, and overcoming

[†] University of Oxford.
[‡] Humboldt-Universität zu Berlin.

(1) Cammack, R.; Frey, M.; Robson, R. *Hydrogen as a Fuel: Learning From Nature*; Taylor and Francis: London and New York, 2001.
(2) Esper, B.; Badura, A.; Roegner, M. *Trends Plant Sci.* **2006**, *11*, 543–549.
(3) Ghirardi, M. L.; Posewitz, M. C.; Maness, P.-C.; Dubini, A.; Yu, J.; Seibert, M. *Annu. Rev. Plant Biol.* **2007**, *58*, 71–91.
(4) Ghirardi, M. L.; King, P. W.; Posewitz, M. C.; Maness, P. C.; Fedorov, A.; Kim, K.; Cohen, J.; Schulten, K.; Seibert, M. *Biochem. Soc. Trans.* **2005**, *33*, 70–72.
(5) Federov, A. S.; Kosourov, S.; Ghirardi, M. L.; Seibert, M. *Appl. Biochem. Biotechnol.* **2005**, *121−124*, 403–412.
(6) Ihara, M.; Nishihara, H.; Yoon, K.-S.; Lenz, O.; Friedrich, B.; Nakamoto, H.; Kojima, K.; Honma, D.; Kamachi, T.; Okura, I. *Photochem. Photobiol.* **2006**, *82*, 676–682.
(7) Hallenbeck, P. C. *Water Sci. Technol.* **2005**, *52*, 21–9.
(8) Ekstroem, J.; Abrahamsson, M.; Olson, C.; Bergquist, J.; Kaynak, F. B.; Eriksson, L.; Sun, L.; Becker, H.-C.; Aakermark, B.; Hammarstroem, L.; Ott, S. *Dalton Trans.* **2006**, 4599–4606.
(9) Hu, X.; Brunschwig, B. S.; Peters, J. C. *J. Am. Chem. Soc.* **2007**, *129*, 8988–8998.
(10) Wilson, A. D.; Newell, R. H.; McNevin, M. J.; Muckerman, J. T.; DuBois, M. R.; DuBois, D. L. *J. Am. Chem. Soc.* **2006**, *128*, 358–366.
(11) Tard, C.; Liu, X.; Ibrahim, S. K.; Bruschi, M.; De Gioia, L.; Davies, S. C.; Yang, X.; Wang, L.-S.; Sawers, G.; Pickett, C. J. *Nature* **2005**, *433*, 610–613.
(12) Cheah, M. H.; Tard, C.; Borg, S. J.; Liu, X. M.; Ibrahim, S. K.; Pickett, C. J.; Best, S. P. *J. Am. Chem. Soc.* **2007**, *129*, 11085–11092.
(13) Darensbourg, D. J.; Reibenspies, J. H.; Lai, C. H.; Lee, W. Z.; Darensbourg, M. Y. *J. Am. Chem. Soc.* **1997**, *119*, 7903–7904.
(14) Rauchfuss, T. B. *Inorg. Chem.* **2004**, *43*, 14–26.
(15) Canaguier, S.; Artero, V.; Fontecave, M. *Dalton Trans.* **2008**, 315–325.
(16) Liu, P.; Rodriguez, J. A. *J. Am. Chem. Soc.* **2005**, *127*, 14871–14878.
(17) Mealli, C.; Rauchfuss, T. B. *Angew. Chem., Int. Ed.* **2007**, *46*, 8942–8944.
(18) Tye, J. W.; Darensbourg, M. Y.; Hall, M. B. *Inorg. Chem.* **2006**, *45*, 1552–1559.
(19) Volbeda, A.; Martin, L.; Cavazza, C.; Matho, M.; Faber, B. W.; Roseboom, W.; Albracht, S. P. J.; Garcin, E.; Rousset, M.; Fontecilla-Camps, J. C. *J. Biol. Inorg. Chem.* **2005**, *10*, 239–249.

10.1021/ja8027668 CCC: $40.75

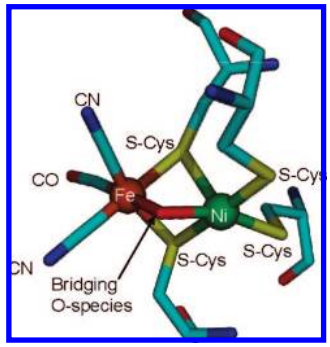

Figure 1. Representation of the active site of *Desulfovibrio fructosovorans* hydrogenase in an oxidized inactive state (Ni−B) with a bridging hydroxide ligand between the Ni and Fe (from the X-ray crystallographic structure determined by Volbeda et al.,[19] PDB code 1YRQ).

this problem is vital if these enzymes (or synthetic catalysts based on their active sites) are to be used in hydrogen cycling technologies.[1,3,23,24]

In general, the highest H_2 production activities are associated with [FeFe] hydrogenases, which have been reported to be particularly sensitive to O_2 (undergoing irreversible inactivation).[23,25] In contrast, rapid H_2 oxidation (uptake) is associated with [NiFe] hydrogenases,[26] which are known to react with O_2 to give one or more inactive states that can be reactivated upon reduction.[24,27,28] The reversibility of O_2 inhibition allows the [NiFe] enzymes to survive in air, and "O_2-tolerant" [NiFe] hydrogenases isolated from knallgas bacteria (such as *Ralstonia*) can even catalyze H_2 oxidation in the presence of O_2.[29–32] We recently demonstrated that the membrane-bound hydrogenase (MBH) from *Ralstonia metallidurans* is able to oxidize trace (<10 ppm) H_2 in air,[33] and we used this enzyme as the anode electrocatalyst in a novel fuel cell able to power a simple electronic gadget from 3% H_2 in air.[34] The basis for O_2 tolerance in hydrogenases is not yet understood; nor is it clear what factors determine whether a hydrogenase should function as a H_2 producer or H_2 oxidizer. Sequence data show that the two hydrogenases that are the subject of this study share 82% identity in the large subunit, which contains the [NiFe] active site, and the amino acids immediately surrounding the active site are identical with those found in the O_2-sensitive periplasmic hydrogenase from *Desulfovibrio gigas*, for which a structure has been determined.[35] The physiological role of *Ralstonia* membrane-bound hydrogenases is in H_2 uptake,[32] but in view of the interest in biological H_2 production for fuels, particularly by microbes engaged in oxygenic photosynthesis, any ability to produce H_2 under aerobic conditions would be an important lead. In this paper we address this issue and show not only that *Ralstonia* [NiFe] hydrogenases are capable of catalyzing H_2 production but also that they can do this continuously in the presence of O_2 and in air itself, provided H_2 is continuously removed.

The technique we use is protein film voltammetry,[36–38] in which a film of enzyme is adsorbed on an electrode surface such that enzyme molecules directly exchange electrons with the electrode and exhibit catalytic activity. This allows detailed investigations of catalysis as a function of potential and other variables that can be altered very easily and precisely within the highly controlled environment of a sealed electrochemical cell. A set of mass-flow controllers providing excellent control of a continuous supply of gas mixtures flowing through the cell completes the hardware. Importantly, the Faradaic current is a sensitive and direct measurement of catalytic rate for a given enzyme film; thus production of H_2 is observed simply as the current due to proton (H^+) reduction, noting that at a bare graphite electrode H^+ reduction is so irreversible as to require a large overpotential (hundreds of millivolts). Protein film voltammetry provides a particularly useful solution to the problem of how to implement and measure H_2 production under aerobic conditions, a situation that is almost unavoidable in H_2 production by oxygenic photosynthesis.[3] In conventional experiments the low-potential electron donors (such as viologens) that are required for H_2 production are oxidized and removed by O_2. In contrast, at an electrode, a continuous supply of electrons can be maintained in the face of O_2; the remaining issue is how to distinguish the current due to enzyme-catalyzed H^+ reduction (H_2 production) from that due to uncatalyzed O_2 reduction. Fortunately, the reduction of O_2 at a graphite electrode is sluggish and there is a large overpotential. Even so, at the elevated O_2 levels in which we are interested, the O_2 reduction current is sufficiently large to overwhelm that due to enzyme action. As we show, this problem can be overcome: H_2 production by the hydrogenase is distinguished easily by introducing a gaseous inhibitor into the oxygenated gas stream and measuring the rapid attenuation and restoration of current as catalysis is first blocked and then recovered as the inhibitor is flushed out.

Methods

Expression systems for *R. metallidurans* CH34 and the *Ralstonia eutropha* C81A mutant will be described elsewhere. The MBH enzymes were all isolated according to the procedure described for *R. eutropha* MBH.[29] The standard reagents NaCl, NaH_2PO_4, and

(20) Jones, A. K.; Sillery, E.; Albracht, S. P. J.; Armstrong, F. A. *Chem. Commun.* **2002**, 866–867.
(21) Karyakin, A. A.; Morozov, S. V.; Karyakina, E. E.; Zorin, N. A.; Perelygin, V. V.; Cosnier, S. *Biochem. Soc. Trans.* **2005**, *33*, 73–75.
(22) Hambourger, M.; Gervaldo, M.; Svedruzic, D.; King, P. W.; Gust, D.; Ghirardi, M.; Moore, A. L.; Moore, T. A. *J. Am. Chem. Soc.* **2008**, *130*, 2015–2022.
(23) Vincent, K. A.; Parkin, A.; Lenz, O.; Albracht, S. P. J.; Fontecilla-Camps, J. C.; Cammack, R.; Friedrich, B.; Armstrong, F. A. *J. Am. Chem. Soc.* **2005**, *127*, 18179–18189.
(24) De Lacey, A. L.; Fernandez, V. M.; Rousset, M.; Cammack, R. *Chem. Rev.* **2007**, *107*, 4304–4330.
(25) Adams, M. W. W. *Biochim. Biophys. Acta* **1990**, *1020*, 115–145.
(26) Vignais, P. M.; Billoud, B. *Chem. Rev.* **2007**, *107*, 4206–4272.
(27) Lamle, S. E.; Albracht, S. P. J.; Armstrong, F. A. *J. Am. Chem. Soc.* **2004**, *126*, 14899–14909.
(28) Lamle, S. E.; Albracht, S. P. J.; Armstrong, F. A. *J. Am. Chem. Soc.* **2005**, *127*, 6595–6604.
(29) Vincent, K. A.; Cracknell, J. A.; Lenz, O.; Zebger, I.; Friedrich, B.; Armstrong, F. A. *Proc. Natl. Acad. Sci. U.S.A.* **2005**, *102*, 16951–16954.
(30) Vincent, K. A.; Cracknell, J. A.; Parkin, A.; Armstrong, F. A. *Dalton Trans.* **2005**, 3397–3403.
(31) Schink, B.; Probst, I. *Biochem. Biophys. Res. Commun.* **1980**, *95*, 1563–9.
(32) Burgdorf, T.; Lenz, O.; Buhrke, T.; van der Linden, E.; Jones, A. K.; Albracht, S. P. J.; Friedrich, B. *J. Mol. Microbiol. Biotechnol.* **2005**, *10*, 181–196.
(33) Cracknell, J. A.; Vincent, K. A.; Ludwig, M.; Lenz, O.; Friedrich, B.; Armstrong, F. A. *J. Am. Chem. Soc.* **2008**, *130*, 424–425.
(34) Vincent, K. A.; Cracknell, J. A.; Clark, J. R.; Ludwig, M.; Lenz, O.; Friedrich, B.; Armstrong, F. A. *Chem. Commun.* **2006**, 5033–5035.
(35) Volbeda, A.; Garcia, E.; Piras, C.; De Lacey, A. L.; Fernandez, V. M.; Hatchikian, E. C.; Frey, M.; Fontecilla-Camps, J. C. *J. Am. Chem. Soc.* **1996**, *118*, 12989–12996.
(36) Vincent, K. A.; Armstrong, F. A. *Inorg. Chem.* **2005**, *44*, 798–809.
(37) Armstrong, F. A.; Heering, H. A.; Hirst, J. *Chem. Soc. Rev.* **1997**, *26*, 169–179.
(38) Vincent, K. A.; Parkin, A.; Armstrong, F. A. *Chem. Rev.* **2007**, *107*, 4366–4413.

Na_2HPO_4 were of analytical grade (Sigma). All electrochemical experiments were carried out in 0.05 M phosphate, together with 0.10 M NaCl as additional supporting electrolyte.[23] Solutions were prepared with purified water (Millipore, 18 MΩ·cm).

Protein film voltammetry experiments were carried out in an anaerobic glovebox (MBraun or Vacuum Atmospheres) comprising a N_2 atmosphere (O_2 < 2 ppm). A pyrolytic graphite edge (PGE) rotating disk electrode (RDE, area 0.03 cm^2) was used in conjunction with an electrode rotator (EcoChemie Autolab RDE) in a specially designed, gastight, glass electrochemical cell that was thermostated using a circulated-water jacket. A saturated calomel reference electrode (SCE) was located in a sidearm containing 0.1 M NaCl that was separated from the main cell compartment by a Luggin capillary and maintained at constant temperature (25 °C). The counter electrode was a piece of Pt wire. Potentials (E) are quoted with respect to the standard hydrogen electrode (SHE) with the correction $E_{SHE} = E_{SCE} + 242$ mV at 25 °C.[39] Electrochemical experiments were carried out using an electrochemical analyzer (Autolab PGSTAT10 or 20) controlled by a computer operating GPES software (EcoChemie). Gases supplied to the headspace of the cell were precisely mixed and provided at a constant flow rate by use of mass flow controllers (Smart-Trak Series 100, Sierra Instruments). These are accurate within 1% of their maximum flow rate; this corresponds to O_2 concentrations of 2% ± 0.25% for the experiment shown in Figure 7A and 21% ± 0.6% for the experiment shown in Figure 7C. The gases used were H_2 (Premier grade, Air Products), O_2 (Air Products), CO (research grade, BOC), argon (BOC), or N_2 (oxygen-free, BOC) or mixtures of these gases. In the experiments where gases were injected as saturated solutions, the concentration in the cell was estimated from the calculated gas concentration, according to Henry's law,[40] in the solution injected.

To prepare an enzyme film, the PGE electrode was first polished for 30 s with an aqueous slurry of α-alumina (1 μm, Buehler) and sonicated for 5 s in purified water, before enzyme solution (1.5 μL, 0.2−1 μg, pH 5.5) was applied and subsequently withdrawn over a period of 10 s. The electrode was then placed in enzyme-free buffered electrolyte so that all enzyme molecules addressed in the experiments were subjected to the same regime of strict potential control. In all experiments the electrode was rotated at a constant rate (2500−6000 rpm) to provide efficient supply of substrate and removal of product.

For experiments carried out under different partial pressures of O_2, it was necessary to estimate the concentration of O_2 that the enzyme molecules at the electrode surface would actually experience, given that a portion of the total dissolved O_2 is actually consumed by the electrode. We therefore carried out a set of quantitative measurements on the electroreduction of O_2 at a bare PGE electrode. Details are given in Supporting Information (Figures S1 and S2), and selected results are included in this paper where relevant.

Results and Discussion

Comparisons of Electrocatalysis under H_2 and N_2. In Figure 2, panels A and B show cyclic voltammograms recorded at a scan rate of 20 mV s^{-1} for a rotating disk electrode modified with wild-type *Ralstonia eutropha* H16 (*Re*) MBH or *Ralstonia metallidurans* CH34 (*Rm*) MBH under conditions of 100% H_2 (approximately 0.8 mM, thick line) or 100% N_2 (thin line) at pH 5.0, 30 °C. We chose pH values in the range 5−5.5 because they are consistent with the pH optimum determined for H_2 oxidation by isolated *Re* MBH.[41] For each enzyme, the voltammograms under N_2 or H_2 were recorded on the same film,

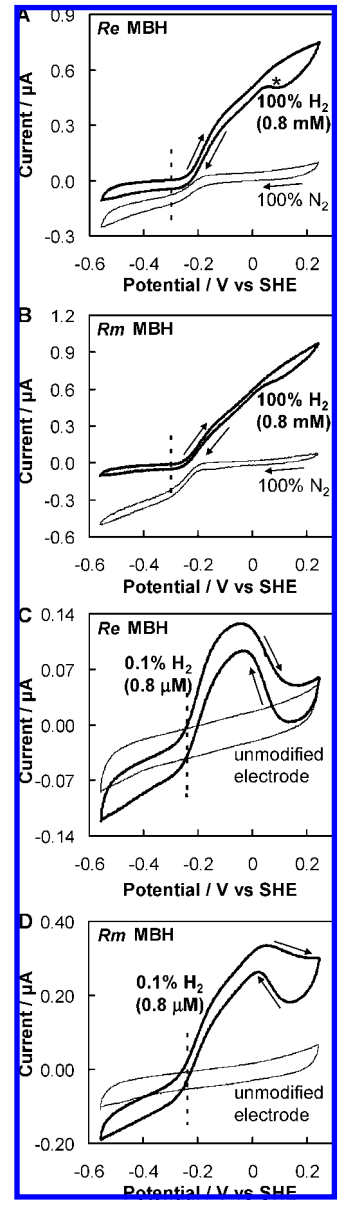

Figure 2. Cyclic voltammograms showing the catalytic bias of (A) *Re* MBH and (B) *Rm* MBH, recorded under 100% H_2 (0.8 mM, thick line) and 100% N_2 (thin line), pH 5.0. Voltammograms for (C) *Re* MBH and (D) *Rm* MBH were recorded under 0.1% H_2 (0.8 μM) in N_2 at pH 5.5. The thin lines in (C) and (D) show the voltammograms for the unmodified electrodes under 0.1% H_2. The trace cuts the axis at the formal potential, showing the reversibility of catalysis at this potential. In all cases, the dashed lines indicate the calculated potential of the $2H^+/H_2$ couple at the H_2 level indicated. Other conditions were 20 mV s^{-1} (A, B) and 10 mV s^{-1} (C, D); 30 °C; electrode rotation rate 3500 rpm (A, B) and 4500 rpm (C, D); electrode surface area 0.03 cm^2; gaseous atmospheres as indicated.

and the cycle under N_2 was recorded first. The time required for gas exchange between the cycles was less than 5 min and film loss was not more than 5% between the scans, so the pair of voltammograms reflects the relative activities (at pH 5.0) for H_2 oxidation at 100% H_2 (0.8 mM) and H_2 production under 100% N_2.

The positive current response seen in the scan recorded under H_2 is due to electrocatalytic H_2 oxidation by the adsorbed enzyme. The voltammogram in this region is complex because as the potential is raised, [NiFe] hydrogenases undergo anaerobic inactivation: this process is reversible (see asterisk in Figure 2A) but inactivation is much more pronounced at low H_2 levels

(39) Bard, A. J.; Faulkner, L. R. *Electrochemical Methods. Fundamentals and Applications*, 2nd ed.; Wiley: New York, 2001.
(40) Dean, J. A. *Lange's Handbook of Chemistry*; McGraw-Hill, Inc.: New York, 1992.
(41) Schink, B.; Schlegel, H. G. *Biochim. Biophys. Acta* **1979**, *567*, 315–324.

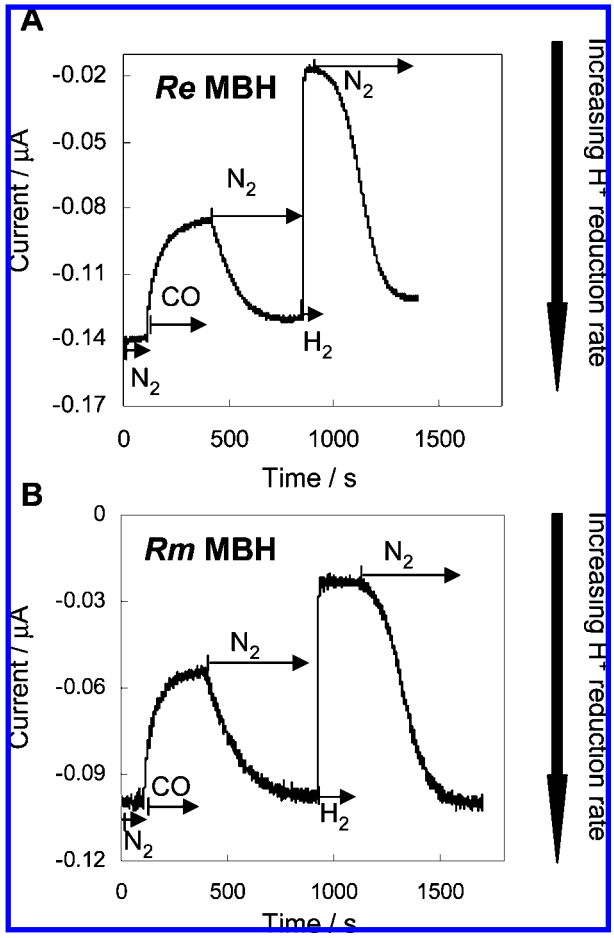

Figure 3. Comparisons of the inhibition of H^+ reduction activities of (A) *Re* MBH and (B) *Rm* MBH by 100% H_2 (0.8 mM) and 100% CO (0.9 mM). Other conditions: −0.45 V vs SHE, pH 5.5, 30 °C, electrode rotation rate 3000 rpm, and electrode surface area 0.03 cm^2.

(see below).[42] In the voltammograms recorded under N_2, the negative current observed at potentials below about −0.2 V corresponds to H^+ reduction (H_2 production), showing that *Re* and *Rm* MBH enzymes both catalyze this reaction. The H^+ reduction current is observed only when the electrode is rotated rapidly to spin away the product, H_2, and if rotation is stopped during H^+ reduction the current response drops rapidly, almost to zero (not shown). No H^+ reduction current is observed in the scans recorded under 100% H_2 (0.8 mM) for either enzyme, indicating that H_2 production is completely inhibited under this condition.

The thermodynamic potential for the $2H^+/H_2$ couple at 100% H_2 (0.8 mM), 30 °C and pH 5.0, is −300 mV as calculated from the Nernst equation, and this value is indicated by the vertical dashed lines on the voltammograms. Based on this standard, and as noted previously for *Re* MBH,[23] there is an overpotential for the onset of H_2 oxidation at 0.8 mM H_2 (approximately 80 mV). Other hydrogenases we have studied do not show this overpotential.[23,38] Under N_2, in the absence of any H_2, the thermodynamic potential for the $2H^+/H_2$ couple is undefined; therefore, to investigate further the overpotential for H_2 oxidation, we carried out experiments at controlled, low partial pressures of H_2. In this way, from a single voltammogram we could measure, simultaneously, the forward and reverse reaction rates as a function of potential for a given pH and H_2 partial pressure. Panels C and D of Figure 2 show voltammograms recorded for *Re* and *Rm* MBH under 0.1% H_2 in N_2 (corresponding to ca. 0.8 μM H_2 in solution) at pH 5.5 and 30 °C. The catalytic current in either case cuts cleanly through the background scans shown for an unmodified electrode, and the zero net current potential (average value of forward and reverse scans) corresponds closely to the thermodynamic potential of the $2H^+/H_2$ couple calculated for this level of H_2 at this pH. A measurable overpotential for H_2 oxidation is thus only apparent at high H_2 levels, a subtlety that is easily quantified by PFV, although its origin remains unclear.

The fact that H^+ reduction (H_2 production) begins at such a high potential shows immediately that the reason these hydrogenases do not evolve H_2 is *not* because there is a problem with overpotential; that is, there is no need to overcome an *electrochemical* activation barrier. In fact the H^+ reduction activity increases rapidly as the potential is scanned in a negative direction through the thermodynamic value but soon reaches a limit at about−0.3 V, suggesting that activity is curtailed by a chemical rate-determining step. (Note that rather than reaching a constant current plateau, the voltammograms show a residual slope, indicative of some dispersion among adsorbed enzyme molecules, some of which are not so well coupled to the electrode.[43])

Comparison of H_2 and CO as Inhibitors of H^+ Reduction. Previously, we investigated the effect of CO on H_2 oxidation by *Re* MBH and were unable to detect inhibition by CO.[29,30] We now describe experiments designed to investigate the effects of CO and H_2 on the H^+ reduction activities of the *Ralstonia* MBH enzymes (Figure 3) and measure the respective inhibition constants $K_I^{app}(CO)$ and $K_I^{app}(H_2)$ for catalysis in this direction. The electrode containing a film of enzyme was poised at a potential at which electrocatalytic H^+ reduction occurs: for pH 5.5 we used −450 mV. At the start of the experiments the cell was subjected to a continuous flow of 100% N_2, and then the headgas was switched to 100% CO (0.9 mM), also under continuous flow. Independent experiments showed that gas exchange under these conditions is essentially complete after 5 min. For both *Re* and *Rm* MBH, the exchange with CO caused the current to decrease. (Since reductive processes yield negative currents, the trace actually rises in the upward direction upon inhibition of H^+ reduction in Figure 3). The current stabilizes after approximately 5 min at about 50% of the initial level. When the gas supply was switched back to 100% N_2, an immediate recovery began, which was complete within the gas exchange time. The gas supply was then switched to H_2. This resulted in a much larger decrease in current, stabilizing almost instantaneously at a value close to zero (in Figure 3 we have not compensated for a small instrumental current offset). When the gas supply was switched back to N_2, there was initially a very slow rate of recovery, which accelerated after approximately 1 min to reach a value similar to that measured at the start of the experiment.

These results are immediately very informative. First, for CO, the slow decrease in current to an intermediate level when CO is added, followed by the contrasting, *immediate* increase in activity when the stream of CO is replaced by N_2, shows that

(42) Jones, A. K.; Lamle, S. E.; Pershad, H. R.; Vincent, K. A.; Albracht, S. P. J.; Armstrong, F. A. *J. Am. Chem. Soc.* **2003**, *125*, 8505–8514.

(43) Léger, C.; Jones, A. K.; Albracht, S. P. J.; Armstrong, F. A. *J. Phys. Chem. B* **2002**, *106*, 13058–13063.

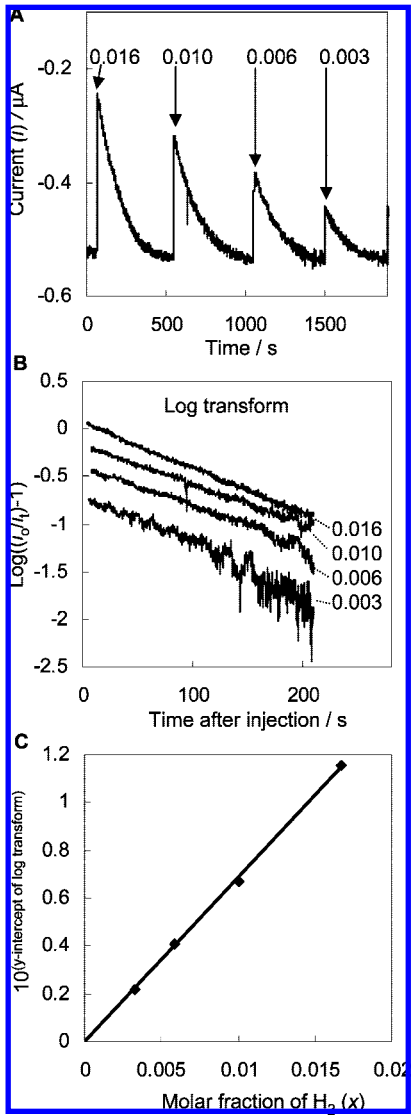

Figure 4. Inhibition of H^+ reduction by H_2. (A) Current transients following the injection of H_2-saturated solutions where the molar fractions of H_2 (x) are as indicated. (B) Log transforms of the current transients shown in panel A for each x value as indicated. (C) Plot of the antilog of the y-intercepts of the individual log transforms with a superimposed line of best fit. Other conditions: 100% Ar atmosphere, 30 °C, pH 5.5, electrode potential −0.45 V, electrode rotation rate 3000 rpm, and electrode surface area 0.03 cm^2.

CO is a weak inhibitor.[44] The inhibition constant $K_I^{app}(CO)$ is evidently so high that the current responds to changes in CO concentration even at levels close to 100%. In fact, an estimate of the value of $K_I^{app}(CO)$ is obtained immediately from the fact that 100% CO (equivalent to just below 1 mM) quenches roughly half the activity. In contrast, when H_2 is flushed into the cell, the loss of current is almost instantaneous and complete; upon changing back to N_2, there is a small lag before the relief of inhibition reaches its maximum rate (the trace is sigmoidal). This reflects the strength of inhibition by H_2 that we noted above; in other words, 100% H_2 (0.8 mM) represents a level so high above the inhibition constant $K_I^{app}(H_2)$, pH 5.5, that the current (catalytic activity) is initially insensitive to its removal. The very similar behavior of *Rm* and *Re* MBH with respect to

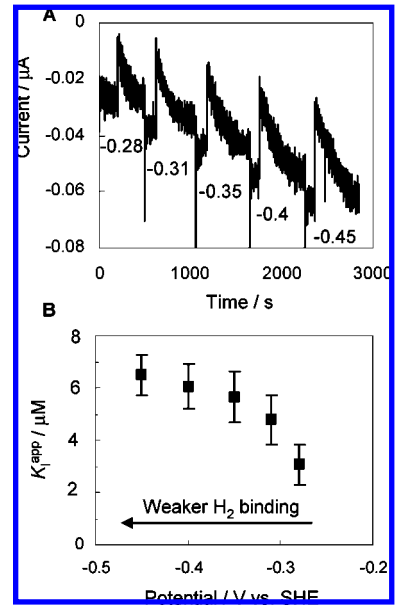

Figure 5. (A) Potential-step chronoamperometric experiments in which *Rm* MBH is subjected to injections of H_2 ($x = 0.008$) at different potentials (in volts) as indicated. (B) Variation in calculated K_I^{app} with potential. Error bars represent estimated accumulated experimental errors. Other conditions: 30 °C, pH 5.5, electrode rotation rate 3000 rpm, and electrode area 0.03 cm^2; carrier gas was 100% Ar.

H_2 being a much stronger inhibitor than CO is in marked contrast with the behavior of the [NiFe] hydrogenase from *Desulfovibrio fructosovorans* (*Df*), for which CO is a stronger inhibitor than H_2.[44]

Experiments to quantify the inhibition of H^+ reduction by H_2 in terms of the apparent inhibition constant [$K_I^{app}(H_2)$, pH 5.5] were conducted by a modification of the procedure introduced by Léger et al.;[44] we note that $K_I^{app}(H_2)$ is an *apparent* inhibition constant because it depends not only on substrate concentration (H^+), and therefore pH, but also on potential (vide infra). The results are interpreted along the lines of that study. Figure 4A shows an experiment in which four consecutive injections of decreasing quantities of H_2-saturated buffer were performed when the electrode was poised, under an Ar atmosphere, at a potential at which H^+ reduction occurs. Immediately after injection the reduction current drops, and then it increases exponentially as the H_2 is flushed out of the cell, eventually returning to its initial level. The log transforms of the data are shown in Figure 4B, from which the y-intercepts are used to calculate $K_I^{app}(H_2)$. The intercepts depend on the molar fraction of inhibitor immediately following each injection (x) as shown in Figure 4C. Values of $K_I^{app}(H_2)$ are summarized in Table 1; for the *Ralstonia* enzymes they are 5−10 times smaller than that reported for the hydrogenase from *Df*.[44] This is a clear manifestation of how tightly inhibitory H_2 is bound by the active site of the *Ralstonia* MBH enzymes.

Inhibition of *Df* hydrogenase by CO was reported to be potential-dependent.[44] Similarly, CO and H_2 inhibition of H^+ reduction by the *Ralstonia* enzymes also depend on potential. Studies of the inhibition by H_2 are presented in Figure 5, in which injections of H_2-saturated buffer were performed at increasingly negative potentials. The trend is similar in appearance to that of *Df* hydrogenase.[44] As the potential becomes more negative, the $K_I^{app}(H_2)$ values increase, that is, binding of inhibitory H_2 becomes weaker. Consequently, the curtailment of the H^+ reduction wave observed in Figure 2(A and B) cannot

(44) Léger, C.; Dementin, S.; Bertrand, P.; Rousset, M.; Guigliarelli, B. *J. Am. Chem. Soc.* **2004**, *126*, 12162–12172.

Table 1. K_I^{app} Values for Inhibition of H_2 Production by H_2 and CO and Their Comparative Importance, Represented as the Selection Factor[a] $K_I^{app}(H_2)/K_I^{app}(CO)$

	Re MBH	*Rm* MBH	*Re* C81A MBH	*Df* hydrogenase
$K_I^{app}(H_2)$, μM	7.1 ± 1.6	10.8 ± 1.2	15.6 ± 5	~166
$K_I^{app}(CO)$, μM	1700 ± 110	1200 ± 60		~5
CO/H_2 selection factor	4×10^{-3}	9×10^{-3}		33

[a] Data for *D. fructosovorans* (*Df*) hydrogenase are taken from ref 44. For *Re*, *Rm*, and *Re* C81A MBH, the conditions were pH 5.5, electrode potential −0.45 V vs SHE, electrode rotation 3000 rpm, 100% Ar, and 30 °C. For *Df* hydrogenase, the temperature was 40 °C and the electrode potential (read from Figure 5 and main text of ref 44) was −0.55 V vs SHE for the $K_I^{app}(H_2)$ measurement and −0.45 V vs SHE for the $K_I^{app}(CO)$ measurement.

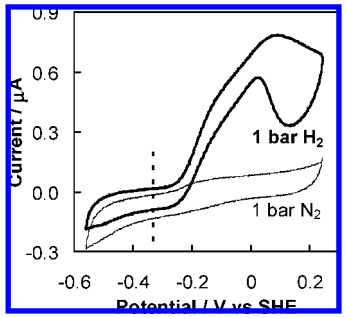

Figure 6. Cyclic voltammograms of the *Re* MBH C81A mutant, which has a low affinity for H_2 in H_2 oxidation, recorded under 100% H_2 (0.8 mM, thick line) and 100% N_2 (thin line). Other conditions: pH 5.5, 30 °C, and electrode rotation rate 2500 rpm.

be due to the onset of increased inhibition by H_2; had this been the case, Figure 5B would show a sharp decrease in K_I^{app} below −0.3 V rather than an increase.

Experiments similar to those shown in Figures 4 and 5 were carried out for CO (Supporting Information, Figures S3 and S4). The $K_I^{app}(CO)$ values are hundreds of times higher than those obtained for inhibition by H_2 and also hundreds of times higher than reported for *Df* hydrogenase.[44] Table 1 includes the CO/H_2 selection factor, which is the ratio of $K_I^{app}(H_2)$ to $K_I^{app}(CO)$: the smaller the selection factor the greater the extent to which H_2 production is inhibited by H_2 compared to CO. As with H_2, potential dependence experiments (Supporting Information, Figure S4) showed that CO is bound more weakly at more negative potential.

Studies of a Mutant Having a High K_M for H_2 Oxidation. The simplest schemes for H_2 production or oxidation by hydrogenases depict a single catalytic cycle common to either direction with H_2 binding or leaving the enzyme, reversibly, in one of its various states.[45] A tightly bound H_2 would thus enhance or inhibit activity depending on the catalytic direction, and intuitively, an enzyme having a high K_M for H_2 oxidation might be predicted to be a good H_2 producer. To explore this possibility within two enzymes of very similar structure, we measured the voltammetry of a mutant form of *Re* MBH (C81A in the large subunit) having a K_M for H_2 oxidation so much higher than the wild-type enzyme[33] that it is not saturated at 100% H_2. As shown in Figure 6, we found that the H^+- reduction activity of the C81A mutant relative to its activity in H_2 oxidation is even lower than for the wild-type enzyme. We measured $K_I^{app}(H_2)$ for the C81A mutant by the method described above and determined that

(45) Armstrong, F. A. *Curr. Opin. Chem. Biol.* **2004**, *8*, 133–140.

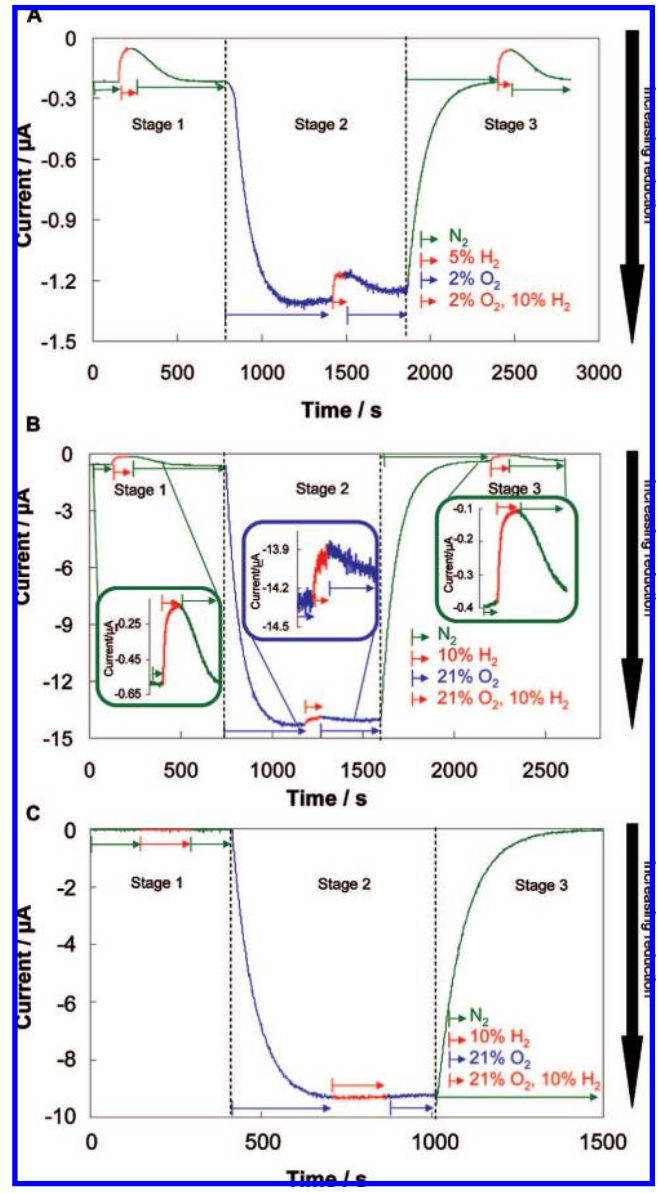

Figure 7. Proof of the capability for H_2 production by *Rm* MBH in the presence of O_2. Control experiment without enzyme present is shown in panel C. Experimental conditions: pH 5.5, potential −0.45 V vs SHE, and electrode rotation rate 3000 rpm; N_2 is the carrier gas throughout the experiment, and the concentrations of H_2 and O_2 indicated are introduced into the head gas. Temperature: (A, C) 30 °C; (B) 40 °C.

this is just slightly higher than the value for the wild-type enzyme (Table 1). Therefore, in this case $K_I^{app}(H_2)$ and K_M for H_2 oxidation have no obvious connection, and other factors in the catalytic cycle determine the catalytic bias within a closely related group of enzymes.

H_2 Production in the Presence of Air. Detecting H_2 production by hydrogenase on a graphite surface is hindered by the fact that although O_2 reduction is sluggish, it occurs over the entire range of potential required for hydrogenase-catalyzed H^+ reduction. Therefore we developed a method to distinguish the contribution to the reduction current arising from enzyme-catalyzed H^+ reduction. The concept involves introducing a gaseous inhibitor of H^+ reduction, which selectively removes the enzyme-catalyzed current component. We have shown above that CO is a poor inhibitor of H^+ reduction by the *Ralstonia* MBH enzymes but that H_2 is a

potent inhibitor. In Figure 7A, an electrode modified with *Rm* MBH is poised at −0.45 V versus SHE. The experiment commences (stage 1) under anaerobic conditions (100% N_2) and the negative current corresponds only to H^+ reduction by the enzyme. After a constant current level was established, the headgas was changed to a mixture of 5% H_2 in N_2 (0.04 mM H_2), which resulted in a rapid loss of current. The headgas was then switched back to 100% N_2 and the H^+ reduction current was slowly recovered. This marked the end of the first stage of the experiment. In stage 2, the headgas was first changed to 2% O_2 in N_2 (20 μM O_2), which resulted in a large increase in current, as expected, due to nonenzymatic O_2 reduction at graphite. At 1400 s the headgas was changed to 2% O_2, 5% H_2, and 93% N_2; that is, a repeat of the first stage except that a constant level of O_2 is maintained. As before, a rapid loss of current is observed, and this is of a similar magnitude to the attenuation observed during the anaerobic stage 1. The headgas was switched back to 2% O_2 in N_2 to remove the inhibitory H_2, and the current recovered. In stage 3, anaerobic conditions were restored by replacing the headgas with N_2. The activity of the enzyme returned to the initial level recorded before O_2 was introduced into the cell, and the gas exchanges of stage 1 were repeated. Figure 7C shows a control experiment on an unmodified electrode, that is, no enzyme, and demonstrates that H_2 has no effect on the O_2 reduction current. In Figure 7A, the similar attenuation of amplitudes in all three inhibition phases therefore show that the H^+ reduction activity of the enzyme is little affected by 2% O_2 in the headgas. A correction factor is required to calculate the actual level of O_2 experienced by the enzyme at the electrode surface due to its electrochemical consumption. As described in Supporting Information, Figure S1, more than 1% O_2 (10 μM) survives under these conditions.

Figure 7B depicts a far more ambitious experiment with 21% O_2 present in the headgas throughout stage 2. This experiment was carried out at 40 °C at which 21% O_2 = 207 μM. The enzyme was inhibited in this case by 10% H_2 (0.8 μM). A similar effect was observed: the crucial attenuation of reduction current upon introduction of H_2 was clearly evident as before, although the trace is more noisy, as observed also for the control experiment shown in Figure 7C. Some activity may be lost during the aerobic phase when H_2 is introduced and then removed, but note also that because >95% of the current is due to O_2 reduction, even a small decrease in this component dominates the result (see the control experiment, where a small change in the O_2 reduction rate is recorded). The final stage of the experiment, measuring the H^+ reduction activity remaining after the aerobic phase, shows that more than 60% of the initial activity remains, and this attenuation could be accounted for simply by film loss. Under the conditions of this experiment, we estimated that at least 13% O_2 (0.14 mM) survives at the electrode to be experienced by the hydrogenase (see Supporting Information, Figure S1). In a final extreme example we looked for H_2 production as 40% O_2 (0.43 mM) was continuously supplied in the headgas, but the trace was too noisy to resolve the current due to enzymatic H^+ production.

A lower limit on the absolute activity of the enzyme can be estimated from eq 1, in which $k_{(E)}$ is the turnover frequency at a potential E, $i_{cat(E)}$ is the current observed at potential E for an electrode rotation rate sufficiently high not to be a variable (i.e., the current is not mass-transport-limited), n is the number of electrons involved in the catalytic reaction, A is the electrode surface area, F is the Faraday constant, and Γ is the electroactive coverage of enzyme.

$$k_{(E)} = \frac{i_{cat(E)}}{nAF\Gamma} \quad (1)$$

If an upper limit of 1×10^{-12} mol cm^{-2} is assumed for Γ,[46] with $n = 2$ and $A = 0.03$ cm^2, a H^+ reduction current of 0.4 μA as obtained in the experiment of Figure 7B corresponds to a lower limit of 70 s^{-1} for H_2 production at −0.45 V, pH 5.5, and 40 °C.

Conclusions

Microbial H_2 production is generally associated with anaerobic as opposed to aerobic organisms, and the O_2 sensitivity of their hydrogenases has been identified as a key problem to be solved. In this respect, since [NiFe] hydrogenases are usually considered to be less prone to O_2 damage than [FeFe] hydrogenases,[25] it follows that photosynthetic organisms expressing [NiFe] hydrogenases (such as cyanobacteria) could actually be more suitable for photosynthetic H_2 farms.[47,48] Our studies of a special class of [NiFe] hydrogenases from aerobic organisms have revealed and quantified several aspects that are relevant to this challenge.

The membrane-bound hydrogenases from *Ralstonia* species, established as H_2-uptake enzymes,[32] produce H_2, but this activity is not normally observed because H_2 is such a good inhibitor. Although our estimate of the lower limit for the turnover frequency k_{cat} is only 70 s^{-1} at pH 5.5 and 40 °C, this value is not so low compared with many enzymes, and it represents a starting point for improvement because a similar rate can be achieved under aerobic conditions (see below). Against this apparent disadvantage in terms of maximum turnover rate, the enzymes display *no significant overpotential* for H_2 production, in contrast to all small analogue active-site mimics so far reported.[12,49,50] Our results with a mutant that has a very high K_M for H_2 oxidation also show conclusively that having a low affinity for H_2 during H_2 oxidation does not necessarily correlate with an improved ability for H_2 production.

To date, the crystal structure of a *Ralstonia* MBH has not been determined, but the sequence relationship with other [NiFe] hydrogenases as well as spectroscopic data[29] indicate that the active site has a very similar coordination environment to that of the enzymes from *D. gigas* and *D. fructosovorans*. One important factor in O_2 tolerance is the rate and potential at which the oxygen-derived inactive state(s) are reactivated. This rescue mechanism is very effective for *Re* and *Rm* MBH and allows them to function in H_2 oxidation under aerobic conditions.[23,33] The same statement should be

(46) This upper limit is estimated on the basis that a higher electroactive coverage should result in the appearance of non-turnover signals due to reversible electron-transfer reactions of the Fe–S clusters when the hydrogenase is inhibited. See: Pershad, H. R.; Duff, J. L. C.; Heering, H. A.; Duin, E. C.; Albracht, S. P. J; Armstrong, F. A. *Biochemistry* **1999**, *38*, 8992–8999.

(47) Cournac, L.; Guedeney, G.; Peltier, G.; Vignais, P. M. *J. Bacteriol.* **2004**, *186*, 1737–1746.
(48) Dawar, S.; Masukawa, H.; Mohanty, P.; Sakurai, H. *Proc. Indian Natl Sci. Acad.* **2006**, *72*, 213–223.
(49) Perra, A.; Davies, E. S.; Hyde, J. R.; Wang, Q.; McMaster, J.; Schroder, M. *Chem. Commun.* **2006**, 1103–1105.
(50) Chong, D. S.; Georgakaki, I. P.; Mejia-Rodriguez, R.; Samabria-Chinchilla, J.; Soriaga, M. P.; Darensbourg, M. Y. *Dalton Trans.* **2003**, 4158–4163.

true for H_2 production, although it is also possible that states of the active site that are engaged in H^+ reduction do not react so rapidly with O_2. The structural factors that lead to O_2 tolerance are clearly very subtle. This is also manifest in the observation that CO is a poor inhibitor of both H_2 oxidation and H^+ reduction, in contrast to other [NiFe] hydrogenases where it is a more potent inhibitor than H_2. It may be that for the enzyme to make the initial distinction between such small substrates and inhibitors, and noting the related metal−ligand bonding characteristics of H_2, O_2, and CO (they are all π-acceptor ligands but coordinate to metal ions in different geometries) the active site stereochemically controls coordination within a tiny space. The most striking result of all is that O_2 is a less potent inhibitor of H_2 production than either H_2 or CO. Thus H_2 can be produced in the presence of at least 10−15% O_2 and this property can be measured in a relatively simple experiment. The results provide a useful benchmark for developing H_2 production by photosynthetic microorganisms.

Acknowledgment. The research of G.G., J.A.C., A.F.W., and F.A.A. was supported by grants from BBSRC (BB/D52222X) and EPSRC (Supergen V). K.A.V. is a Royal Society Research Fellow. The research of M.L., O.L., and B.F. was supported by the Sfb 498 (Project C1) and the Cluster of Excellence 'Unifying Concepts in Catalysis' funded by the Deutsche Forschungsgemeinschaft.

Supporting Information Available: Experimental details, Supporting Figures S1−S4, and Supporting Equations S1−S6. This material is available free of charge via the Internet at http://pubs.acs.org.

JA8027668